



Dysfunctional cerebrovascular tone contributes to cognitive impairment in a non-obese rat model of prediabetic challenge: Role of suppression of autophagy and modulation by anti-diabetic drugs

Walaa Fakh^{a,1}, Ali Mroueh^a, Houssein Salah^b, Ali H. Eid^a, Makram Obeid^{b,c}, Firas Kobeissy^d, Hala Darwish^{e,*}, Ahmed F. El-Yazbi^{a,f,*}

^a Department of Pharmacology and Toxicology, Faculty of Medicine, American University of Beirut, Beirut, Lebanon

^b Department of Anatomy Cell Biology and Physiology, Faculty of Medicine, American University of Beirut, Beirut, Lebanon

^c Division of Child Neurology, Department of Pediatric and Adolescent Medicine, American University of Beirut Medical Center, Lebanon

^d Department of Biochemistry and Molecular Genetics, Faculty of Medicine, American University of Beirut, Beirut, Lebanon

^e Hariri School of Nursing, American University of Beirut, Beirut, Lebanon

^f Department of Pharmacology and Toxicology, Faculty of Pharmacy, Alexandria University, Alexandria, Egypt

ARTICLE INFO

Keywords:

Prediabetes
Cerebral artery tone
Cognitive impairment
Hippocampal inflammation

ABSTRACT

Prediabetes is a highly prevalent stage of early metabolic dysfunction that poses a high risk for cardiovascular and cognitive impairment without a clear pathological mechanism. Here, we used a non-obese prediabetic rat model previously developed in our laboratory to examine this mechanism. These rats were subjected to a mild metabolic challenge leading to hyperinsulinemia without hyperglycemia or obesity. This was associated with impaired hippocampal-dependent cognitive functions together with an augmented cerebrovascular myogenic tone. Consequently, hippocampal expression of hypoxia-inducible factor-1 α increased, together with markers of mitochondrial dysfunction and oxidative stress. In parallel, the phosphorylation of Akt and mTOR increased in the prediabetic rat hippocampus alongside increased expression of p62 and LC3 puncta indicating a possible repression of autophagic flux. Neuroinflammation and neuronal apoptosis were detected in the hippocampal CA1 area as increased CD68 and IBA-1 staining, as well as increased TUNEL staining and caspase-3 activity, respectively. Treatment with metformin or pioglitazone, at a previously determined vasculoprotective non-hypoglycemic dose, reversed the cerebrovascular and hippocampal molecular alterations and ameliorated cognitive function. The present study proposes a mechanistic framework whereby prediabetic cerebrovascular impairment potentially leads to a mild hypoxic state that is exacerbated by the metabolic dysfunction-driven suppression of neuronal autophagy leading to cognitive impairment.

1. Introduction

Type 2 diabetes represents a global pandemic with projected steep rises in incidence and prevalence over the next 20–30 years [1]. This was brought about by lifestyle and environmental changes [2], specifically pertaining to an increased intake of refined diets low in fiber and rich in sugars and saturated fat [3]. With considerable health impact, the detrimental outcome of these metabolic disorders is not only restricted to increased risk of cardiovascular mortality and morbidity [4], but also accelerated cognitive decline [5]. Interestingly, research

findings showed that indicators of both vascular and cognitive dysfunction could co-exist in the prediabetic stage preceding the diagnostic features of type 2 diabetes [6].

Prediabetes represents an early stage of metabolic impairment characterized by insulin resistance and glucose intolerance, with an increased risk of vascular complications [7]. While evidence supports a clear role for diabetes as a risk factor for cognitive decline [8], results regarding the prediabetes-associated risk had been less conclusive, with studies implicating prediabetes [9], and others failing to establish an association [10]. However, recent evidence from large longitudinal and

* Corresponding authors at: Department of Pharmacology and Toxicology, Faculty of Medicine and Medical Centre, American University of Beirut, P.O. BOX 11-0236, Riad El-Solh 1107 2020, Beirut, Lebanon (A.F. El-Yazbi); Hariri School of Nursing, American University of Beirut, Beirut, Lebanon (H. Darwish).

E-mail addresses: hd30@aub.edu.lb (H. Darwish), ae88@aub.edu.lb (A.F. El-Yazbi).

¹ Current address: INSERM UMR1260 Regenerative NanoMedicine, Fédération de Médecine Translationnelle de Strasbourg, Université de Strasbourg, Faculté de Pharmacie, 67401 Illkirch, France.

<https://doi.org/10.1016/j.bcp.2020.114041>

Received 13 February 2020; Accepted 14 May 2020

Available online 19 May 2020

0006-2952/ © 2020 Elsevier Inc. All rights reserved.

cross-sectional population-based studies implicated this disorder in the development and progression of cognitive impairment in humans. A nine-year cohort study showed that prediabetic patients with slightly elevated but sub-diagnostic glycosylated hemoglobin (HbA1c) levels, had an accelerated decline in cognitive function, assessed by the Mini-Mental State Examination, compared to metabolically healthy individuals [5]. Moreover, a large cross-sectional study showed that non-diabetic patients with impaired fasting or post-prandial blood glucose scored worse on cognitive function tests compared to control subjects [11]. Specifically, non-diabetic individuals with insulin resistance showed reduced cognitive performance, memory, and executive function compared to metabolically healthy individuals [12]. Several mechanisms link hyperglycemia to the development of neuronal inflammation and cognitive impairment, including increased neuronal polyol pathway flux, increased advanced glycation end-product-mediated neuronal injury, increased protein kinase C activity, and increased reactive oxygen species production [13]. In addition, the blood-brain barrier leakiness seems to contribute to neuronal inflammation in advanced metabolic dysfunction including diabetes and obesity [14]. However, the mechanisms through which cognitive dysfunction develops during prediabetes and insulin resistance are far less clear, albeit a vascular component had been suggested [5,12].

On the other hand, metabolic dysfunction is associated with a reduction of cerebral blood flow to the extent observed in patients with Alzheimer's dementia [15]. Interestingly, these cerebrovascular abnormalities known to lead to cognitive decline are not only common in diabetes [16], but also occur in the prediabetic stage [17], where insulin resistance contributes to endothelial dysfunction and increased cerebrovascular tone [6]. Indeed, a number of previous studies reported increased cerebrovascular tone in animal models of prediabetes and insulin resistance [18,19] potentially contributing to chronic yet mild cerebral ischemia.

Whereas metabolic disease accelerates cognitive decline, activation of neuronal autophagy reverses the age-related memory deficits [20]. Autophagy is a process of self-digestion whereby the cellular machinery recycles misfolded proteins and dysfunctional organelles, an essential activity in quiescent terminally differentiated neuronal cells [21]. A considerable body of evidence implicates the reduction of autophagy in the pathogenesis of neurodegenerative disease and associated cognitive impairment [22–25]. Interestingly, several studies showed that autophagy is suppressed in metabolic disorders with insulin resistance in the liver [26], and muscle [27]. As well, there has been no paucity of evidence linking insulin resistance to increased protein aggregates in the brain [28,29], even in the absence of hyperglycemia [30], yet the contributory role of autophagy and the effects of its potential suppression or activation remain largely unknown.

As such, we hypothesized that prediabetic metabolic dysfunction could lead to cognitive impairment via altering cerebrovascular and neuronal autophagic functions. Whereas increased cerebrovascular tone would limit blood supply and initiate hypoxic damage, suppression of autophagy potentially aggravates the insult by reducing neuronal turnover of damaged organelles/molecules. To study this, we examined the cognitive and cerebrovascular functions of a rat model developed in our laboratory by exposure to a mild metabolic challenge [31–33]. These rats fed a mild hypercaloric diet demonstrate increased serum insulin, dyslipidemia, and adipose inflammation without an increase in body weight, hyperglycemia, or hypertension following twelve weeks of feeding on this diet. Nevertheless, progressive loss of fasting and random blood glucose control occurs after 16 weeks of exposure to mild hypercaloric diet leading to development of significant hyperglycemia indicative of type 2 diabetes by 24 weeks. Perivascular adipose inflammation in this rat model triggers vascular dysfunction with increased contractility, endothelial dysfunction, and increased vascular oxidative stress [31–33]. In the present study, we extended our investigation to examine the impact of this early metabolic dysfunction on cerebrovascular tone and cognitive function. Our results showed

that endothelial dysfunction and increased cerebrovascular tone in this model were associated with signs of hippocampal hypoxia, mitochondrial dysfunction, suppression of autophagy, and increased hippocampal inflammation and apoptosis. This was coupled with a cognitive deficit that was ameliorated by treatment with metformin or pioglitazone, as examples of anti-diabetic drugs used to treat insulin resistance.

2. Methods

2.1. Ethical approval

All animal experiments performed in this study were conducted as per an animal protocol approved by the American University of Beirut Institutional Animal Care and Use Committee and are in accordance with the Guide for Care and Use of Laboratory Animals issued by the National Academy of Science [34].

2.2. Animal treatment

Forty Male Sprague-Dawley rats (4–5 weeks of age; \approx 150 g) were allocated randomly to four treatment groups (10 rats per group) and kept for 12 weeks: (1) Control group receiving normal chow (ENVIGO, Teklad Rodent Diets, Madison, WI) providing 3 kcal/g, (2) MHC group receiving mild hypercaloric diet providing 4.035 kcal/g, (3) MHC-met group receiving MHC diet and treated with 100 mg/kg metformin at week 10, (4) MHC-pio group receiving MHC diet and treated with 2.5 mg/kg pioglitazone at week 10. Rats were caged individually in a standard controlled environment. Daily calorie intake was recorded and MHC diet was prepared according to the recommendations of the American Institute of Nutrition (AIN-93M) [35] as described previously [32,33]. All rats were handled for 2 min by the experimenters and habituated to the housing, testing room, and the empty Y maze used for cognitive testing for a total of 5 min daily, 5 consecutive days before the experiment. Drug treatment was performed as described previously [33]. Animals were fasted overnight prior to sacrifice. At the time of sacrifice, animals from each group were alternated between three different protocols: injection of Evans Blue dye, transcardiac perfusion and fixation, or brain collection for dissection for myography and flash freezing of dissected hippocampus in liquid nitrogen.

Three additional groups of six rats were used for pilot and confirmatory experiments. Two groups were used in parallel as control and MHC-fed groups kept for 24 weeks to ascertain the development of hyperglycemia at this time point in order to confirm the prediabetic nature of our rat model. The third group was fed control diet for 8 weeks and then switched to MHC diet for four weeks to determine if the change in dietary composition was associated with cognitive effects that preceded the development of the metabolic changes.

2.3. Nuclear magnetic resonance

LF10 Minispec Nuclear Magnetic Resonance (NMR) machine (Bruker, MA, USA) was used to measure rat fat/lean ratio to detect different tissue densities. The values obtained from each rat are compared to a standardized, calibrated rat.

2.4. Behavioral testing

Previous studies reported an early deficit in hippocampal-dependent functions upon metabolic challenge preceding these observed in functions related to other brain centers [36,37]. The cognitive tests used in this study, to assess hippocampal-dependent function, require motor and muscle coordination, therefore we assessed the rats motor power using an accelerating rotarod test as described previously to rule out any deficits [24]. The latency to fall, revolutions per minute of falling, and distance traveled on the rod were recorded, and the average value obtained from the four trials of the second test day was used for

analysis.

2.4.1. Spontaneous object recognition using Y-maze

Hippocampal-dependent recognition memory was assessed using a test of spontaneous novel object recognition in a Y-maze as described previously [38,39]. Briefly, the rats were habituated to the empty maze for 1 min, 5 days before the test. The test was conducted over 2 trials, 2 min each, with 15 min inter-trial delay. The rat was placed in the middle arm of the maze and allowed to explore freely. During the first trial (learning phase), two identical objects were placed equidistantly in the right and left arms of the maze (A, A'). During the second trial (discrimination trial), the familiar object in the left arm was replaced with a novel object (B). The maze and objects were wiped with 70% ethanol between trials to eliminate odor build-up. Novelty preference scores were calculated based on the time spent exploring the different objects as indicated previously [38]. The time spent by each animal touching, sniffing, or turning around each object with head directed towards the object not more than 2 cm radius was considered exploration time.

2.4.2. Morris water maze (MWM)

Spatial learning and memory (acquisition and recall) were assessed using the MWM test as previously described [39,40]. A circular plastic pool 1.5 m in diameter) was filled with 25 °C water. At least 3 spatial cues visible to the rats were kept constant in the room, with the experimenter standing in the same location throughout the testing period. On the first testing day, considered a habituation day, rats were allowed to swim for 2 min freely. During the spatial acquisition trials on days 2–5, an “invisible platform” was placed 2 cm below the water surface in the Northeast Quadrant (Platform Quadrant). Rats were placed in the pool at four different equidistant immersion sites (north, east, south, and west). If a rat failed to find the platform in 2 min, the experimenter guided and placed the animal on it for 30 s. Immersion landmarks sequence was changed every day. On testing day 6, the platform was removed, and rats were introduced to the maze starting at a position across from the platform quadrant. Rats were allowed to swim freely for 2 min to assess spatial memory. Monitoring of the ability of the rats to swim to a visible platform was done on the last day to assess their motor and visual functions. The animals were dried and kept in their home cages in the testing room between trials.

The Spontaneous object recognition test preceded the Morris Water Maze test. All behavioral tests were video recorded and analyzed with the automated SMART Video Tracking software (Panlab, Holliston, MA) with the camera suspended above the testing fields

2.5. Assessment of blood-brain barrier leakiness

Two percent Evans Blue dye solution in physiological saline was filtered and injected intraperitoneally at a 4 ml/kg dose to each rat 24 h before sacrifice [41]. At sacrifice, rats were subjected to transcardiac perfusion with 50 ml of ice-cold PBS then brain tissue was removed and divided into right and left hemispheres. The left hemisphere was weighed and snap-frozen in liquid nitrogen then stored at –80 °C. To extract and quantify the amounts of Evans Blue dye in brain tissue, the left hemisphere was homogenized in 2 ml ice-cold PBS then sonicated for 20 min (30-s on, 30-s off). Samples were then centrifuged at 14,000 rpm for 10 min at 4 °C. Equal volumes of the supernatant were added to 60% trichloroacetic acid (TCA) solution. Samples were placed on a rotor for 1 h at 4 °C and then centrifuged at 14,000 rpm for 10 min at 4 °C. A PBS blank and a duplicate of each sample (200 µL) were added to a 96-well plate then the fluorescence was measured using TriStar² S LB 942 Multimode Reader (Bethold, Bad Wildbad, Germany) at an excitation and emission wavelengths of 485 nm and 530 nm, respectively. To serve as a positive control, the same test was conducted on a group of 3 rats that were rendered diabetic after 8 weeks of HFD feeding by a single intravenous injection of streptozotocin injection

(40 mg/kg) dissolved in citrate buffer. Their diabetic status was confirmed by random blood glucose measurement showing weekly readings consistently above 300 mg/dl.

2.6. Pressure myography

Rat middle cerebral arteriole segments were set up for pressure myography experiments as described previously [33]. In pressure ramp experiments, the pressure was dropped to 10 mm Hg after myogenic tone development and then gradually raised in a series of steps to 10, 20, 40, 60, 80, 100, 120, 140 mm Hg. The outer diameter of the vessel was measured at each pressure point. The pressure was then dropped back to 10 mm Hg and the vessel was washed and kept in a calcium-free buffer containing (NaCl 130 mM, KCl 4 mM, MgSO₄·7H₂O 1.2 mM, NaHCO₃ 4 mM, HEPES 10 mM, KH₂PO₄ 1.18 mM, Glucose 6 mM, EDTA 0.03 mM, EGTA 2 mM, pH 7.4) and the ramp was repeated. Active tone was calculated as the difference in the outer diameter of the middle cerebral artery when in calcium-containing and calcium-free buffer at the respective pressure points. To establish the active tone in denuded vessels, a small air bubble was flushed through the vessel. A lack of response to acetylcholine (ACh) was used to confirm loss of endothelium, then the experiment was performed as mentioned.

To evaluate the endothelial function, following stable myogenic response development, arteries were kept at 80 mm Hg pressure and increasing concentrations of ACh (10⁻⁹–10⁻⁵ M) were added to the bath in a semi-log manner. The outer diameter following each dose of ACh was measured and endothelium-dependent dilation was established as the difference in diameter compared to baseline diameter at 80 mm Hg.

2.7. Blood glucose levels, HbA1c, and glucose tolerance testing:

Blood glucose levels and oral glucose tolerance testing were done as described previously [31] in blood droplets collected by a tail prick using Accu-check Performa glucometer (Roche Diagnostics, Rotkreuz, Switzerland). HbA1c levels were measured in blood samples obtained from the tail vein at the end of the feeding period using a bench-top Labona Check A1c analyzer (Greencross Medis, Cheonan-Si, South Korea) as per the manufacturer's instructions. The insulin resistance index (HOMA-IR) values were calculated using fasting blood glucose and insulin levels as described previously [42].

2.8. Blood chemistry

Blood samples were collected after decapitation and centrifuged at 5000 rpm for 5 min at 4 °C. Serum was stored at –80 °C. Total serum leptin, adiponectin and insulin were measured using rat leptin, rat adiponectin, and rat insulin ELISA kits (Thermo-Fisher Scientific, Waltham, MA) as per protocols supplied by the manufacturer

2.9. Brain fixation and sectioning

Rats were anesthetized with a ketamine/xylazine mixture (up to 80 mg/kg body weight ketamine, and 10 mg/kg body weight xylazine) after which they were subjected to transcardiac perfusion with 100 ml ice cold PBS, followed by 100 ml 4% paraformaldehyde. Brains were then isolated and paraffin imbedded. Later, serial sections of 8 µm thickness were prepared and used for different staining techniques. Owing to the importance of the CA1 area of the hippocampus in spatial memory [43] and detection of novelty [44] in rats, fields from this area were used for the collection of data for the different staining techniques.

2.10. DHE staining

Fixed brain tissue samples were stained with 20 µM

dihydroethidium (Invitrogen, Carlsbad, CA). Red fluorescence representing reactive oxygen species (ROS) was captured using LEICA DM6 B fluorescence imaging microscope, through the Alexa Fluor 568 filter.

2.11. TUNEL assay

Terminal deoxynucleotidyl transferase dUTP nick end labeling (TUNEL) staining was performed using Click-iT Plus TUNEL Assay kit (Thermo-Fisher Scientific, Waltham, MA) following the manufacturer's instructions. Nuclei were stained with 300 nM DAPI solution in phosphate-buffered saline for 5 min. Images were taken using LEICA DM6 B fluorescent microscope (Leica Biosystems, Buffalo Grove, IL) through the Alexa Fluor 647 filter.

2.12. Immunohistochemistry

Fixed brain tissue samples were used for immunohistochemistry as described previously [31,32]. Briefly, hippocampal sections were incubated with either 1:500 rabbit polyclonal CD68 antibody (Abcam, Cambridge, UK) or 1:1000 recombinant anti-Iba1 antibody (Abcam, Cambridge, UK) overnight at 4 °C. Immunoreactivity was developed using Novolink polymer Detection Kit (Leica Biosystems, Buffalo Grove, IL). Images were taken using OLYMPUS CX41 light microscope (Olympus, Shinjuku, Tokyo, Japan).

2.13. Immunofluorescence

Fixed brain tissue samples were used for immunofluorescence as described previously [45]. Briefly, slides were incubated overnight at 4 °C with 1:200 rabbit polyclonal anti-LC3B (Novus Biologicals, Centennial CO). The next day slides were washed and incubated with 1:100 mouse monoclonal NeuN antibody (EMD Millipore, Burlington, MA) for 2 h at room temperature. A mixture of 1:1000 Texas red-conjugated goat anti-rabbit IgG and 1:1000 Alexa Fluor 488-conjugated goat anti-mouse IgG (Abcam, Cambridge, UK) for 1 h at room temperature. Nuclei were stained with 300 nM DAPI solution in phosphate-buffered saline for 5 min. Images were taken using LEICA DM6 B fluorescent microscope (Leica Biosystems, Buffalo Grove, IL).

2.14. Caspase-3 activity assay

After decapitation, hippocampus tissue samples were used to quantify Caspase-3 activity using a fluorometric assay kit (Abcam, Cambridge, UK) as indicated by the supplier. The signal was quantified using TriStar² S LB 942 Multimode Reader (Bethold, Bad Wildbad, Germany) at an excitation and emission wavelengths of 400 and 505 nm, respectively.

2.15. Western blot

Protein extraction and Western blotting were performed as described previously [46]. Membranes were incubated in primary antibody in 0.1% TBST (1:1000 rabbit polyclonal phospho-Akt (T308), 1:1000 rabbit polyclonal SQSTM1/p62 antibody, 1:1000 rabbit polyclonal SIRT3, and 1:1000 rabbit polyclonal HIF-1 alpha antibody, from Abcam (Cambridge, UK); 1:1000 rabbit polyclonal Phospho-mTOR (Ser2448) antibody, 1:1000 rabbit polyclonal Phospho-DRP1 (Ser616) antibody, and 1:2000 rabbit monoclonal GAPDH, from Cell Signaling Technology (Danvers, MA) overnight at 4 °C. After washing with 0.02% TBST (4 × 5 min), membranes were incubated in 1:40,000 biotin-conjugated goat anti-rabbit Ig (Abcam, Cambridge, UK) for 1 h at room temperature followed by washing and incubation with 1:60,000 horse radish peroxidase conjugated streptavidin (Abcam, Cambridge, UK) for 30 min at room temperature. Blots of the GAPDH were developed using 1:5000 horse radish peroxidase-conjugated goat anti-rabbit secondary

antibody (Abcam, Cambridge, UK). Clarity Western ECL substrate (BioRad, Hercules, CA) was used to generate signal image detection using ChemiDoc imaging system (BioRad, Hercules, CA). Band optical density was quantified using ImageJ software and normalized to GAPDH.

2.16. Statistical analysis

Data were expressed as mean ± standard error of the mean. Statistical significance was tested using *t*-test, one-way ANOVA, or two-way ANOVA followed by the appropriate *post hoc* test as indicated in the corresponding section in the results or the figure legends using GraphPad Prism software version 7. *P* value < 0.05 was considered statistically significant.

3. Results

3.1. MHC diet feeding leads to a prediabetic metabolic state

MHC-fed rats consumed ~15 kcal/day more than their control counterparts (data not shown). While this did not reflect in an increased body weight for the 12-week feeding duration (Fig. 1A), an increased fat/lean ratio was observed indicative of adipose expansion (Fig. 1B). However, neither an increase in random blood glucose level (Fig. 1C) nor in glucose tolerance (Fig. 1D) was detected. Similarly, no increase in HbA1c levels was seen at 12 weeks of feeding but increases indicative of increased blood glucose levels were observed in rats fed MHC diet for 24 weeks (Fig. 1E). Yet, an increased serum insulin concentration (Fig. 1F) and insulin resistance index (HOMA-IR, Fig. 1G) confirmed the hyperinsulinemic prediabetic state previously reported in this model. Interestingly, despite the observed change in body composition, there was no significant alteration of serum levels of leptin (Fig. 1H) or adiponectin (Fig. 1I). On the other hand, no change in blood glucose level or fat/lean ratio were observed in the rat group fed MHC diet for four weeks (data not shown).

3.2. Cerebrovascular, motor, and cognitive consequences of MHC diet feeding

Middle cerebral artery segments from MHC-fed rats showed an augmented myogenic response (Fig. 2A & B). The arterioles from MHC-fed rats showed an increased active tone compared to those from control rats in the operational pressure range of the rat cerebral artery (Fig. 2C). As well, middle cerebral arterioles from MHC fed rats showed endothelial dysfunction manifesting as a reduction in the ACh-mediated vasodilation. Whereas vessel segments from control rats demonstrated a concentration-dependent dilation of the myogenic tone by ACh, this response was much attenuated in segments from MHC-fed rats (Fig. 2D & E). Interestingly, abolishing the vascular endothelial feedback by denuding the cerebral vessel segments equalized the active tone production in vessel segments from control and MHC-fed rats (Fig. 2F). On the other hand, MHC feeding did not affect blood-brain barrier leakiness measured as the absorption of Evans blue dye in the brain. Compared to control, MHC-fed rats did not show an increased Evans blue penetration, whereas rats rendered diabetic by receiving STZ injection showed a four-fold increase (Data not shown).

On the level of motor function, MHC-fed rats did not show a deficit in the accelerating rotarod test. Latency to fall (Control: 64.64 ± 7.71 s; MHC: 70.03 ± 10.73 s; *n* = 10, *P* > 0.05), distance traveled on the rotarod (Control: 185.9 ± 31.15 cm; MHC: 203.5 ± 38.16 cm; *n* = 10, *P* > 0.05), and maximum velocity reached (Control: 13.58 ± 0.84 rpm; MHC: 14.17 ± 1.22 rpm; *n* = 10, *P* > 0.05) were not different between the MHC-fed and control rats. However, cognitive hippocampal-dependent functions including novel object recognition and spatial learning and memory appeared to be affected negatively by the mild metabolic dysfunction

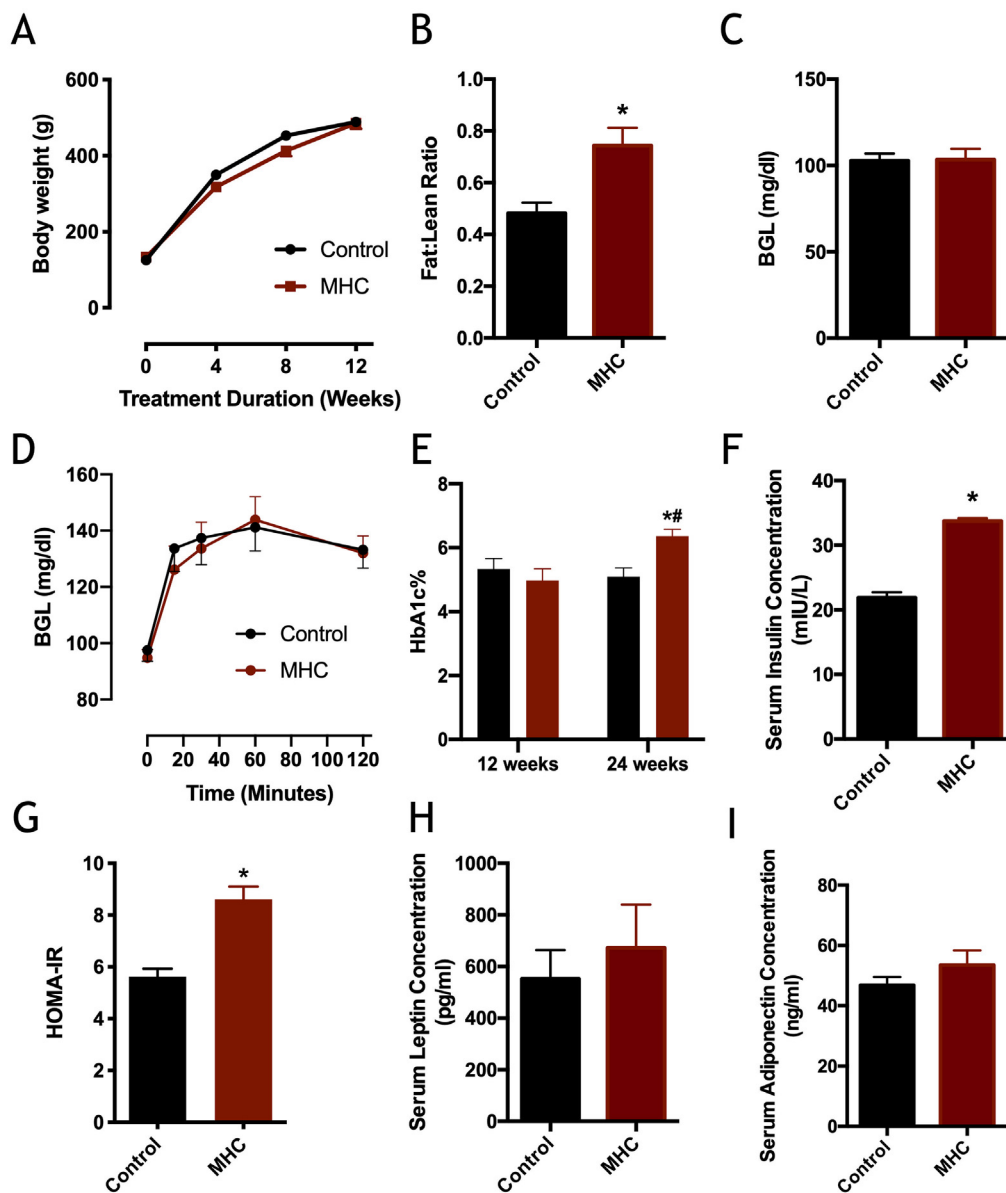


Fig. 1. Metabolic consequences of 12 weeks of MHC-feeding. A, Time course of change in body weight ($n = 10$); B, body composition represented as fat/lean ratio ($n = 10$); C, random blood glucose level ($n = 10$); D, oral glucose tolerance test ($n = 6$); E, HbA1c levels at 12 and 24 weeks of MHC feeding ($n = 6$); F, serum insulin levels ($n = 10$); G, insulin resistance index ($n = 10$); H, serum leptin ($n = 10$); and I, serum adiponectin concentrations after 12 weeks of feeding in control and MHC-fed rats. Data summarized represent results from n rats per group. Statistical analysis was done by two-way ANOVA followed by Sidak's multiple comparisons test For A ($F(1,18) = 3.54$ for the treatment factor, treatment \times time interaction term ($3,54) = 3.11$) and D ($F(1,10) = 0.1$ for the treatment factor, treatment \times time interaction term ($4,40) = 0.2$), while for B, C, E-I, unpaired t -test was used. * denotes $P < 0.05$ vs. control rats.

induced by twelve weeks of MHC feeding. Both control and MHC-fed rats were able to learn the location of the rescue platform over time, demonstrated by a progressive reduction in the latency to reach platform along the successive spatial acquisition trial days of the MWM test (Fig. 2G). However, compared to controls, MHC-fed rats were slower in reaching the escape platform with significantly longer escape latencies on the second to fourth day of testing. Moreover, acquisition of place learning plateaued at a minimum on the third testing day in controls, while MHC-fed rats continued to learn at a slower pace throughout the 5 testing days. In the Probe trial, MHC-fed rats exhibited retention demonstrated by a reduced preference for the platform quadrant, spending less time in the designated area (Fig. 2H & I). Similarly, the MHC rats showed a reduced novelty preference score indicating an impaired recognition function compared to control animals (Fig. 2J & K). Interestingly, none of the cognitive deficits observed in rats receiving MHC diet for 12 weeks were seen at the early feeding time point of four weeks, whose results in MWM and Y-maze were not different from control rats (data not shown).

3.3. Metformin or pioglitazone treatment reverses cerebrovascular and behavioral deficits in MHC-fed rats

Similar to our previous findings [31,32], a two-week treatment of MHC-fed rats with non-hypoglycemic doses of metformin or pioglitazone did not alter blood glucose levels (Fig. 3A), but only pioglitazone reduced serum insulin levels (Fig. 3B). As well, the cerebrovascular myogenic tone was restored to control levels (Fig. 3C), together with the vasodilatory response to ACh (Fig. 3D). These metabolic and cerebrovascular changes were associated with reversal of behavioral dysfunction as well. MHC-fed rats treated with metformin or pioglitazone demonstrated a restoration of the spatial memory with an increased preference of the platform quadrant in the Probe Trail in MWM test (Fig. 3E). Moreover, object novelty preference scores were restored to control values in MHC-fed rats receiving metformin or pioglitazone (Fig. 3F).

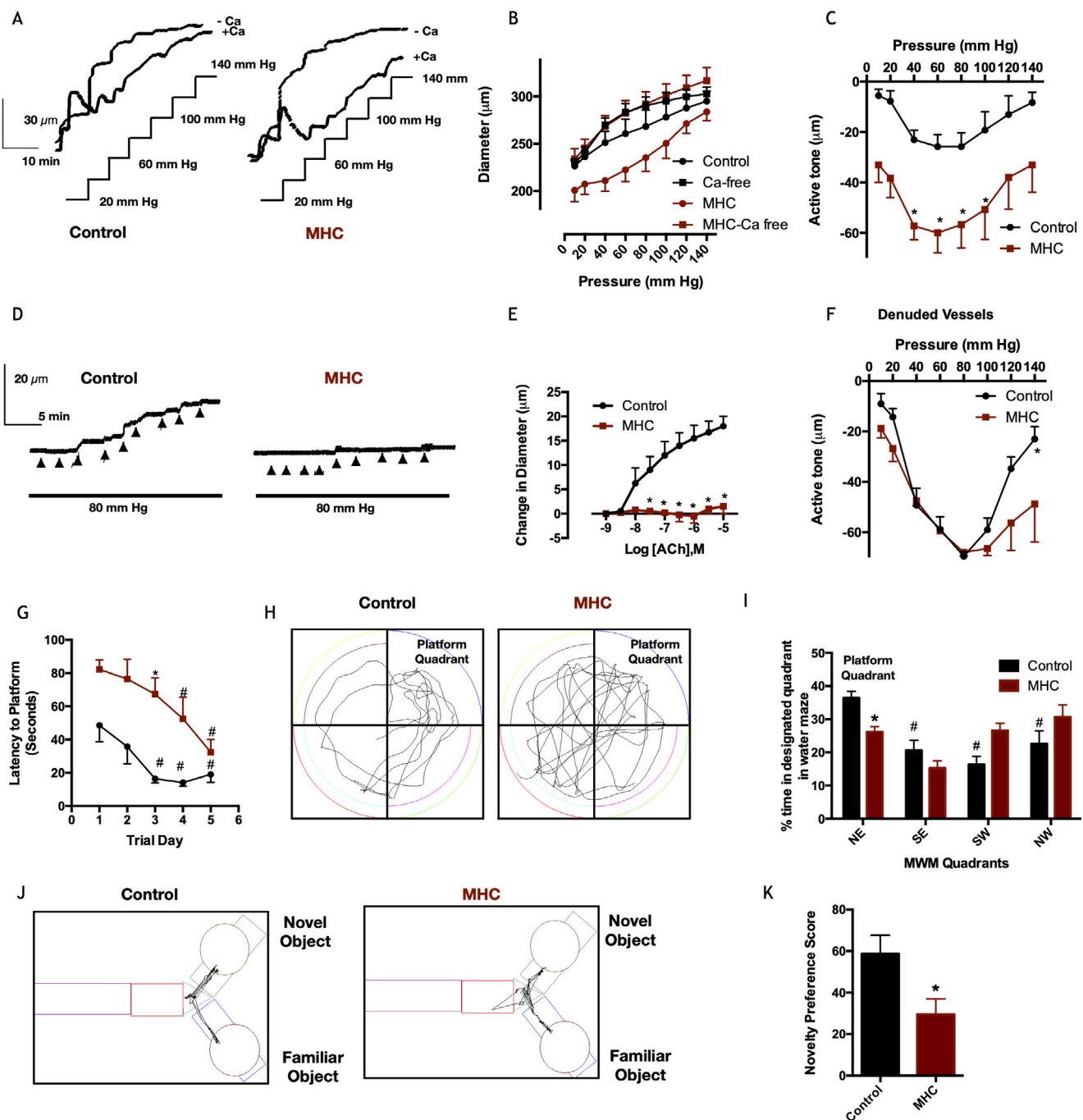


Fig. 2. Cerebrovascular tone and endothelial and cognitive functions in control and metabolically challenged rats. A, Representative tracings of pressure myography experiments depicting changes in rat middle cerebral artery diameter as a function of change in intravascular pressure in vessel segments from control (left) and MHC-fed (right) rats in presence (+ Ca) and absence (- Ca) of calcium in the bath solution; B, summary of the change in middle cerebral artery diameter as a function of pressure change ($n = 4$); C, Active tone generated by rat middle cerebral artery in vessel segments from control and MHC-fed rats. Active tone is the difference in diameter of the vessel at a given intravascular pressure value in absence and presence of calcium ($n = 4$); D, Representative tracings of the endothelium-dependent vasodilatory effects of increasing ACh concentrations in rat middle cerebral artery segments producing stable myogenic tone during pressurization to 80 mm Hg from control (left) and MHC-fed rats (right); E, Increase in rat middle cerebral artery diameter in response to increasing ACh concentrations ($n = 4$); F, Active tone generated by rat middle cerebral artery segments after endothelium denudation ($n = 4$); G, Latency to platform on in different training days in MWM test in control and MHC-fed rats ($n = 10$); H, Representative tracings of rat activity in MWM probe trial; I, Time spent by control or MHC-fed rats in different quadrants in the probe trial of MWM test ($n = 10$); J, Representative tracings of rat activity in Y-maze test; K, Novelty preference score for control and MHC-fed rats in novel object recognition test in the Y-maze ($n = 10$). Data summarized represent results from vessel segments from n different rats per group. Statistical analysis was done by two-way ANOVA followed by Sidak's multiple comparisons test For B ($F(1,6) = 2.95$ for treatment factor, treatment \times pressure interaction term (7,42) = 1.5), C ($F(1,6) = 17.08$ for treatment factor, treatment \times pressure interaction term (7,42) = 0.2), E ($F(1,6) = 24.83$ for treatment factor, treatment \times Ach concentration interaction term (8,48) = 15.15), F ($F(1,6) = 4.06$ for treatment factor, treatment \times pressure interaction term (7,42) = 1.85), G ($F(1,18) = 9.83$ for treatment factor, treatment \times pressure interaction term (4,72) = 1.58), and I ($F(1,18) = 4.54$ for treatment factor, treatment \times position interaction term (3,54) = 5.06), while for K unpaired t -test was used. * denotes $P < 0.05$ vs. the corresponding value in control rats, while # denotes $P < 0.05$ vs. the latency value on the first training session or the control value in the NE quadrant for G and I, respectively.

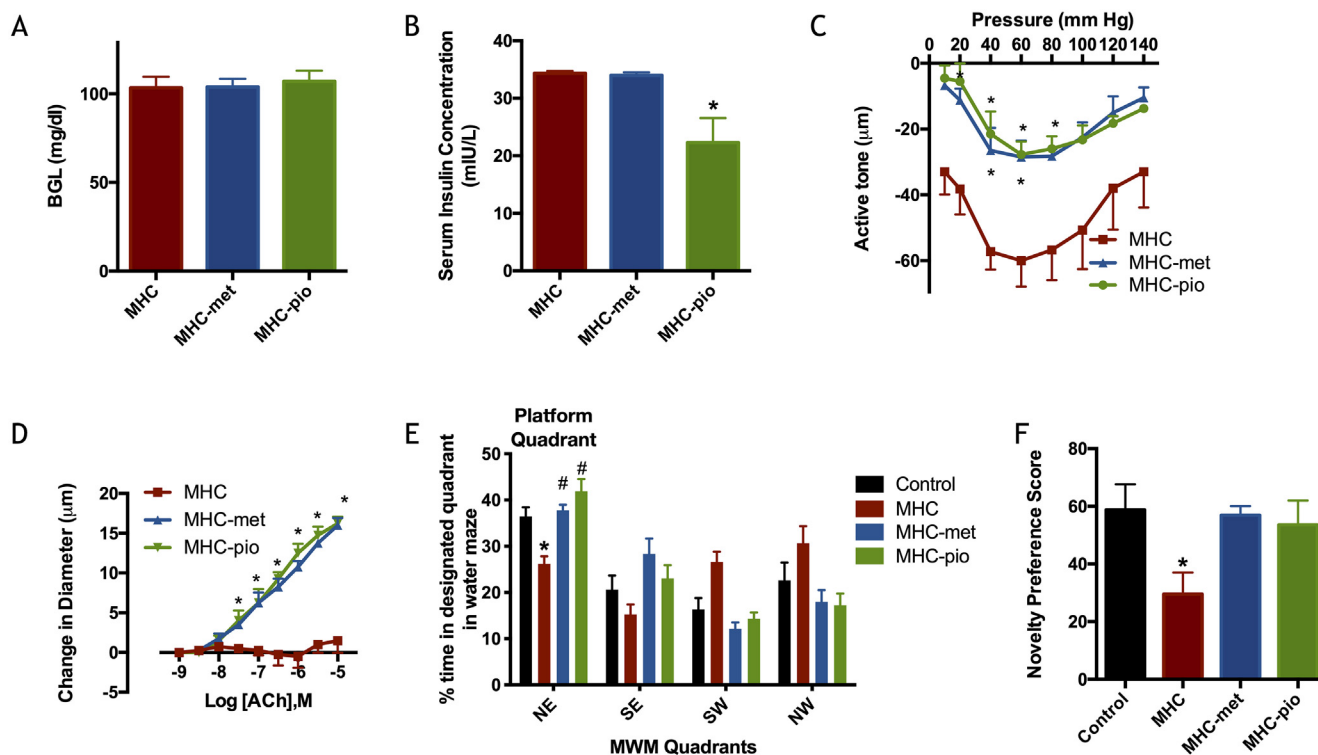


Fig. 3. Metformin and pioglitazone treatment reversed cerebrovascular and cognitive deficits in MHC-fed rats. A, Random blood glucose level ($n = 10$); B, serum insulin level ($n = 10$); C, active myogenic tone of rat middle cerebral artery ($n = 4$); D, ACh-mediated endothelium-dependent dilation of middle cerebral artery ($n = 4$); E, time spent in different quadrants in MWM ($n = 10$); and F, novelty preference score in novel object recognition in Y-maze test ($n = 10$) in MHC-fed rats with or without a two-week oral treatment with non-hypoglycemic doses of metformin or pioglitazone. Data summarized represent results from n rats per group. Statistical analysis was done by one way ANOVA followed by Tukey multiple comparisons test For A ($F(2,27) = 0.13$), B ($F(2,27) = 30.28$), and F ($F(3,36) = 3.42$), and by two-way ANOVA followed by Sidak's multiple comparisons test for C ($F(2,9) = 14.56$ for treatment factor, treatment \times pressure interaction term ($14,63) = 0.36$), D ($F(2,9) = 35.31$ for treatment factor, treatment \times Ach concentration interaction term ($16,72) = 24.67$), and E ($F(3,36) = 2.13$ for treatment factor, treatment \times position interaction term ($9,108) = 5.92$). * denotes $P < 0.05$ vs. the corresponding value in control rats.

3.4. MHC feeding is associated with increased markers of hippocampal hypoxia, mitochondrial dysfunction and oxidative stress reversed by metformin or pioglitazone

Consistent with the presumed hypoxic impact of the chronic reduction of brain perfusion due to an increased cerebrovascular tonic contraction in MHC-fed rats, HIF-1 α expression level increased in the hippocampus (Fig. 4A). This was associated with increased markers of mitochondrial dysfunction and oxidative stress. Increased phosphorylation of dynamin-related protein 1 (DRP1) at Ser616, the site enhancing DRP1-mediated mitochondrial fission and increased ROS production, was observed in the hippocampus of MHC-fed rats (Fig. 4B). No change in total DRP expression was observed among the different groups (Data not shown). Additionally, the expression levels of the mitochondrial deacetylase, sirtuin3 (Sirt3), was reduced in the hippocampus of MHC-fed rats (Fig. 4C). Along the same lines, DHE staining showed that hippocampal ROS levels increased in MHC-fed rats compared to controls (Fig. 4D). Interestingly, metformin or pioglitazone treatment attenuated mitochondrial dysfunction markers and ROS staining levels in MHC-fed rats to values not significantly different from controls.

3.5. MHC feeding is associated with decreased hippocampal autophagy restored by metformin or pioglitazone treatment

In order to investigate whether the hyperinsulinemic state induced by MHC feeding affected autophagy in rat hippocampus, a number of relevant markers were examined. Akt activity increased in MHC-fed rat hippocampus as indicated by elevated phosphorylation at Thr308

compared to control rats (Fig. 5A), alongside a concomitant increase in the mammalian target of rapamycin (mTORC1) phosphorylation at the Akt-dependent site, Ser2448 [47] (Fig. 5B). No changes in total Akt and mTORC1 expression were detected among the different groups (Data not shown). This was accompanied by an increase in the expression level of the adaptor protein p62 in MHC-fed rats (Fig. 5C). Moreover, double immunofluorescence staining of the hippocampal neurons in the CA1 area demonstrated an increased LC3B puncta in MHC-fed rat sections (Fig. 5D). In line with its effect on metabolic, vascular, and mitochondrial dysfunction parameters, treatment with either metformin or pioglitazone ameliorated the observed increases in the Akt and mTORC1 phosphorylation, p62 expression, and LC3B puncta in MHC-fed rat hippocampus.

3.6. MHC feeding triggers hippocampal inflammation and apoptosis that is reversed by metformin or pioglitazone treatment

Both CD68 and IBA1 staining showed increased microglial activation in the CA1 area consistent with increased inflammation (Fig. 6A–C). Increased inflammation in this area was associated with elevated apoptotic cell death. Increased hippocampal neuron apoptosis in MHC-fed rats was evident as increased TUNEL staining in the hippocampal CA1 area compared to control rats (Fig. 6A & D) and an increased caspase-3 activity in total hippocampal lysates as measured in fluorimetric activity assays (Fig. 6E). Consistent with the other functional and molecular observations, both hippocampal microglial activation and apoptosis were reduced in metformin or pioglitazone treated MHC-fed rats.

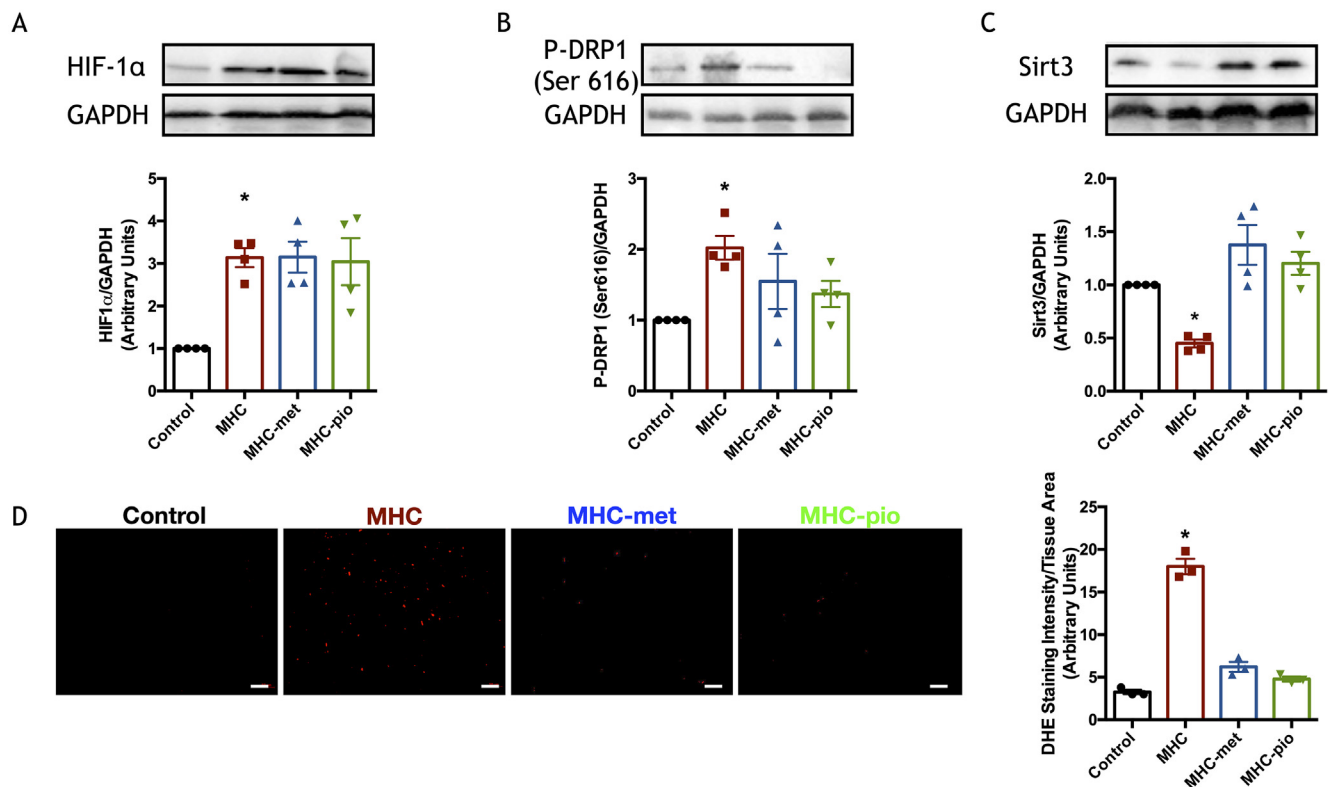


Fig. 4. Increased markers of hypoxia, mitochondrial dysfunction, and oxidative stress in metabolically challenged rat hippocampus recovered after treatment. A, HIF-1 α expression; B, Ser616 DRP1 phosphorylation; and C, Sirt3 expression levels. Western blots shown are representative of four separate experiments on extracts from four different rats per group summarized in the bar graphs. D, DHE staining in hippocampus from control, MHC-fed, and MHC-fed rats treated for two weeks by either metformin or pioglitazone. DHE staining appears as red fluorescence on the representative micrographs. Scale bars are 50 μ m. DHE data are a summary of nine sections from three different rats per group summarized in the bar graph. Statistical analysis was done by one-way ANOVA followed by Tukey multiple comparisons test ($F(3,12) = 9.1$, $F(3,12) = 3.38$, $F(3,12) = 13.46$, and $F(3,8) = 134$ for A, B, C, and D, respectively). * denotes $P < 0.05$ vs. the corresponding value in control rats. (For interpretation of the references to color in this figure legend, the reader is referred to the web version of this article.)

4. Discussion

Early metabolic dysfunction poses a significant health risk despite not meeting the diagnostic cut-off criteria for full-blown metabolic disorders. Prediabetes in particular, with a global prevalence estimate ranging from 35 to 50% [48], poses a considerable health burden owing to the associated metabolic, cardiovascular, and cognitive decline [5,7]. As such, a careful investigation of the unique mechanisms linking early metabolic challenge with cognitive decline is warranted in order to allow optimal intervention. Here, we examine the potential detrimental pathways linking prediabetic metabolic perturbation to cognitive impairment in a non-obese rat model of mild metabolic challenge. Our results suggest that early metabolic challenge induces cerebrovascular dysfunction that leads to chronic hypoperfusion and hypoxia. Such a hypoxic state co-exists with a suppression of neuronal autophagy possibly driven by metabolic impairment culminating in neuronal inflammation and apoptotic cell death in the hippocampus.

In the present study, early metabolic challenge was induced by a mild hypercaloric diet feeding. Our rat model receives ~38% of dietary calories from fat, in slight excess of the upper limit of dietary fat intake recommended by the American Diabetes Association (20–35%) [49]. Fructose was added to represent refined sugars, which together with saturated fat, are thought to be the cause of cardiovascular abnormalities in humans and animal models associated with western diets [50]. In our previous work [32,33], the MHC rat model developed a prediabetic metabolic impairment manifested as hyperinsulinemia without an increase in neither blood glucose levels nor body weight after 12 weeks of MHC feeding. This rat model represents the earliest stage of diabetes pathogenesis where insulin secretion is increased to achieve a

normal blood glucose level [51]. It is noteworthy that fasting and random hyperglycemia became detectable in this rat model by the 24th week of exposure to MHC [32] indicating that the impairment observed at 12 weeks represent a *bona fide* prediabetic state. This was further confirmed in the present study where MHC rats developed hyperinsulinemia and insulin resistance, possibly driven by a change in body composition favoring increased fat/lean ratio, without a change blood glucose level or body weight enabling the examination of vascular and cognitive dysfunction at an early stage of metabolic deterioration. Once more, the prediabetic nature of the MHC model was emphasized by the increased HbA1c levels seen at the end of 24 weeks of feeding.

As expected, MHC-fed rats demonstrated an impaired hippocampal-dependent cognitive function. Both novelty recognition and spatial memory acquisition and recall were reduced compared to control rats. This occurred without an effect on motor function as demonstrated in the rotarod test indicating that the observed deficit is more likely to be cognitive rather than a consequence of alteration of motor activity. The lack of change in cognitive function at the early time point of 4-week MHC feeding, alongside the absence of changes in body composition, suggests that the observed deficit after 12 weeks is the results of metabolic impairment rather than a direct consequence of a dietary compositions change. Significantly, adipose expansion observed here as an increased fat/lean ratio, together with the perivascular adipose inflammation consistently demonstrated in this rat model [31,32], might suggest that the cognitive decline develops due to an altered adipokine profile. Indeed, obesity-associated increases and decreases in circulating levels of leptin and adiponectin, respectively, are thought to mediate cognitive decline [52]. However, this did not appear to be the case in our model, since no change was detected in serum levels of

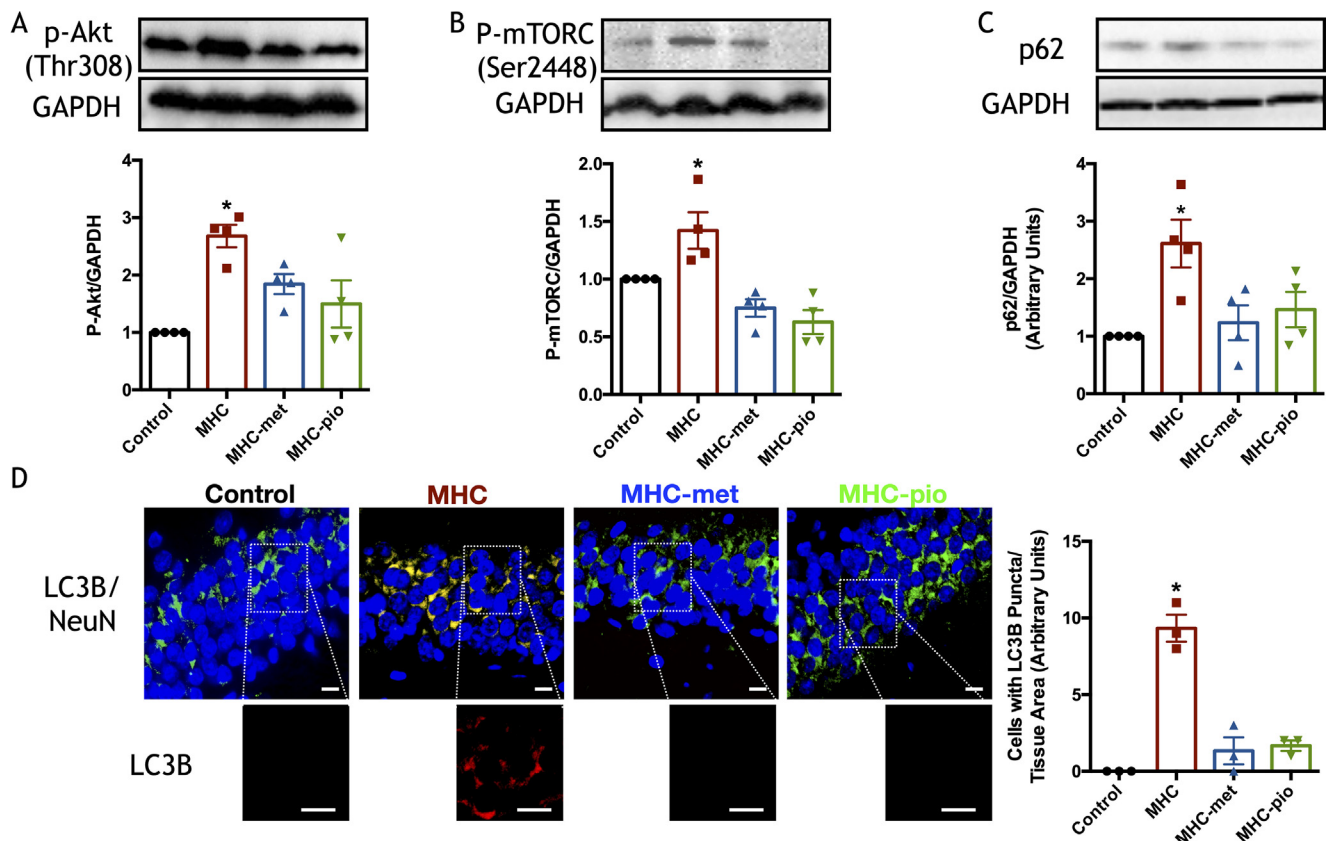


Fig. 5. Activation of the Akt/mTORC pathway and decreased autophagy in hippocampus in metabolically challenged rats reversed by treatment. A, Akt phosphorylation at Thr308; B, mTORC phosphorylation at Ser2448; and C, p62 expression levels. Western blots shown are representative of four separate experiments on extracts from four different rats per group summarized in the bar graphs. D, LC3 puncta in hippocampus from control, MHC-fed, and MHC-fed rats treated for two weeks by either metformin or pioglitazone. NeuN staining appears as green fluorescence, LC3 staining appears as red fluorescence, while DAPI nuclear staining appear as blue fluorescence on the representative micrographs. Cells expressing both NeuN and LC3 show yellow fluorescence in the merged image. Scale bars are 5 μ m. Immunofluorescence data are a summary of nine sections from three different rats per group summarized in the bar graph. Statistical analysis was done by one-way ANOVA followed by Tukey multiple comparisons test ($F(3,12) = 8.44$, $F(3,12) = 11.82$, $F(3,12) = 5.69$, and $F(3,8) = 42.91$ for A, B, C, and D, respectively). * denotes $P < 0.05$ vs. the corresponding value in control rats. (For interpretation of the references to color in this figure legend, the reader is referred to the web version of this article.)

either adipokine in MHC-fed rats.

On the other hand, late stages of metabolic dysfunction including obesity and diabetes were shown to be associated with significant impairment of cognitive functions related to the hippocampus as a result of increased blood-brain barrier leakiness leading to neuronal inflammation [14]. Yet our rat model of early metabolic challenge did not demonstrate an increased blood-brain leakiness similar to that observed in the rat group in which type 2 diabetes was induced by streptozotocin injection. This is consistent with previous studies showing that hippocampal-dependent cognitive function impairment was detected in rats fed a western diet prior to an increase in blood-brain barrier leakiness and body weight [37]. As such, alternative explanations for the observed cognitive impairment were sought.

Indeed, our previous observations in this prediabetic rat model showed increased vascular contractile tone and endothelial dysfunction as a consequence of perivascular adipose inflammation and mild metabolic dysfunction [32,33]. This was a consequence of an enhanced smooth muscle calcium sensitization downstream of increased basal RhoA-dependent kinase activity. An augmented vascular tone was consistently observed in other prediabetic rat models as well [18]. Cerebral arterioles are among the resistance vessels producing a spontaneous myogenic contractile response in face of increasing pressure. Such a response is crucial for the maintenance of several functions including blood flow autoregulation, tissue protection, and modulation of oxygen and nutrient delivery according to regional metabolic needs

[53]. Our previous study examining endothelial function in several vascular beds in MHC rats indicated a reduced endothelial-dependent hyperpolarization in cerebral arterioles resulting from inward rectifier potassium channel dysfunction [33] without a change in endothelial nitric oxide synthase expression or phosphorylation [32,33]. Here, we extended the investigation of cerebrovascular reactivity to show that the endothelial deficit caused MHC-fed rat middle cerebral arterioles produced an elevated myogenic response over the operational range of the blood vessel. Literature suggests that mean blood pressure in rat middle cerebral artery is ~ 60 mm Hg [54], which is the values associated with the largest difference in active tone production between vessel segments from control and MHC-fed rats in pressure myography experiments. As expected, ACh-mediated endothelium-dependent relaxation of rat middle cerebral arteriole was impaired in vessel segments from MHC-fed rats. Interestingly, upon removal of the endothelial layer, denuded cerebral arteriolar segments from both control rats produced increased myogenic constriction equivalent to that generated by segments from MHC-fed rats. This indicated that augmented myogenic response observed in vessels from metabolically impaired rats is potentially due to a reduced endothelial feedback.

Owing to increased cerebral arteriole myogenic tone and reduced vessel diameter at physiological pressures, cerebral hypoperfusion and hypoxia become probable consequences in MHC-fed rats. This was confirmed by the elevated expression of HIF-1 α in MHC-fed rat hippocampus. Indeed, similar changes in HIF-1 α expression were seen

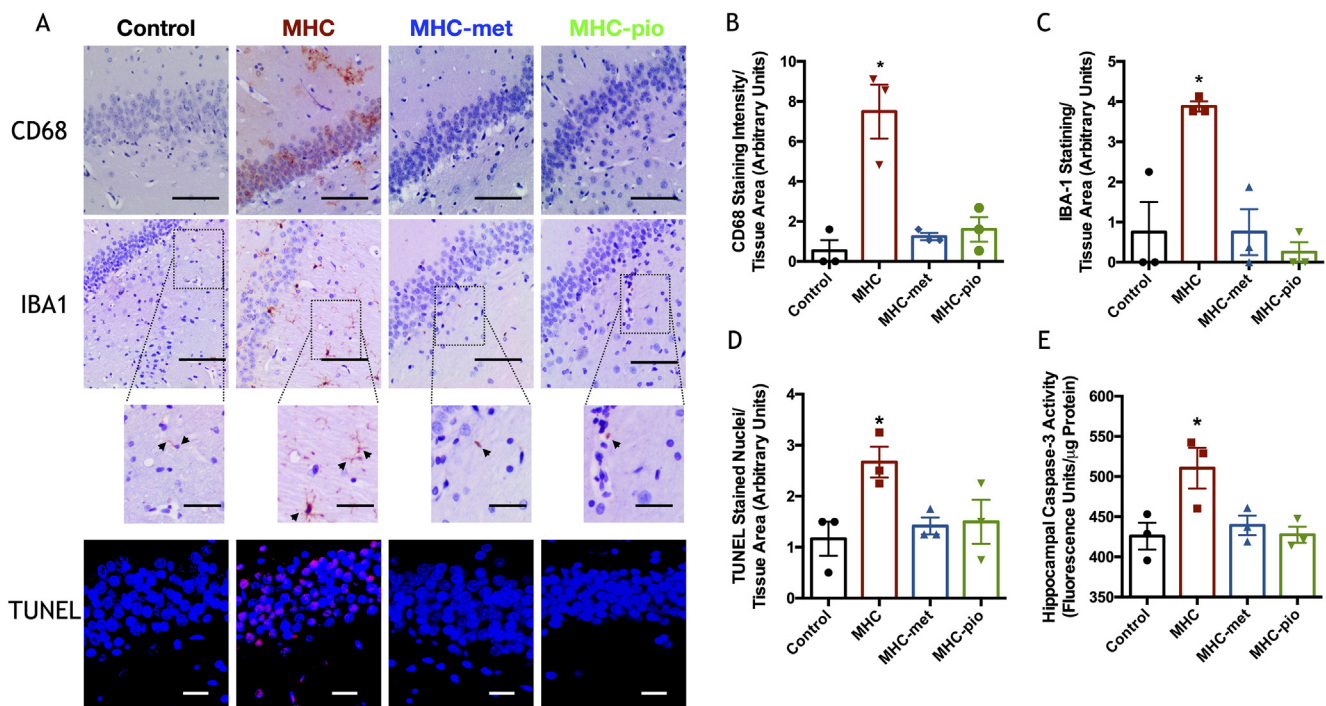


Fig. 6. Increased microglial activation and apoptosis in hippocampus in metabolically challenged rats reversed by treatment. A, Representative micrographs of CD68, IBA-1, and TUNEL staining in CA1 area of rat hippocampus with the corresponding quantification in B, C & D, respectively. CD68 and IBA-1 staining appear as brown color on a background of H&E staining, while TUNEL staining appear as red fluorescence together with the blue fluorescence of DAPI nuclear staining on the representative micrographs. Scale bars are 25 μ m and 10 μ m for the insets on the IBA-1 panels. Microscopy data are a summary of nine sections from three different rats per group. E, Caspase-3 activity normalized to the hippocampal extract protein concentration ($n = 3$). Statistical analysis was done by one-way ANOVA followed by Tukey multiple comparisons test ($F(3,8) = 14.53$, $F(3,8) = 11.41$, $F(3,8) = 4.28$, and $F(3,8) = 5.52$ for B, C, D and E, respectively). * denotes $P < 0.05$ vs. the corresponding value in control rats. (For interpretation of the references to color in this figure legend, the reader is referred to the web version of this article.)

accompanied by a decline in hippocampal-associated memory following intermittent hypoxia [55]. Consistent with the literature showing that cerebral hypoxia and accumulation of HIF-1 α are associated with increased ROS levels [56], MHC-fed rat hippocampus demonstrated a high oxidative burden upon DHE staining. Moreover, mitochondrial dysfunction is a common occurrence in hypoxic neuronal injury [57]. As such, we proceeded to examine two mitochondrial markers; DRP1 phosphorylation at Ser616 promoting mitochondrial fission [58], and Sirt3 that plays a role in maintaining mitochondrial antioxidant function and biogenesis [59]. Studies have shown that hypoxia triggered a feedback mechanism downregulating mitochondrial activity through increased fragmentation, mitophagy, and reduced biogenesis [60,61]. Specifically, recent studies reported that hypoxia-induced mitochondrial fission via increased HIF-1 α expression leading to increased DRP1 activity [62–64]. This was indeed the case in the hippocampus of MHC-fed rats where increased DRP1 phosphorylation at Ser616 was observed. Furthermore, as previously observed in HFD-fed mice showing cognitive dysfunction [65], Sirt3 expression levels were reduced in MHC-fed rat hippocampus.

In the context of neuronal injury, evidence showed that cells respond to increased mitochondrial fission by triggering autophagy [61,66] as a quality control mechanism to clear damaged mitochondrial segments [67,68]. Indeed, autophagy activation was reported to have a neuroprotective role, not only in neurodegenerative disease [24,69], but also under hypoxic conditions [70,71]. Yet, this did not appear to be the case in MHC-fed rats. In line with the early metabolic challenge manifesting as hyperinsulinemia, the hippocampus of MHC-fed rats showed increased Akt phosphorylation at Thr308. This in turn was associated with an increased mTORC phosphorylation at the Akt sensitive site, Ser2448 [47]. Multiple lines of evidence implicate the activation of the insulin receptor/Akt/mTORC signaling pathway in suppression of autophagy associated with insulin resistance in neurons

[72] and peripheral tissue [73]. mTORC activation represses the activity of the unc-51-like kinase 1 (ULK1) via phosphorylation, and thus precludes autophagosome maturation [74]. Additionally, recent findings revealed an additional mechanism whereby ULK1 inhibition contributes to autophagy suppression through prevention of autophagosome and lysosome fusion [75]. In this context, MHC-fed rat hippocampus showed accumulation of the adaptor protein SQSTM1/p62 and increased LC3 puncta in neuronal cells in the CA1 area indicative of an impeded autophagy flux. Interestingly, studies of CA1 neurons of Alzheimer's patients showed a similar picture [76].

In parallel, examination of the hippocampus in rats with early metabolic challenge revealed an increase in markers of inflammation and apoptosis. On the one hand, MHC-fed rats showed increased expression of CD68 and IBA-1, both markers of microglial activation associated with chronic neuroinflammation [77], in the CA1 area of the hippocampus. On the other hand, increased apoptotic changes in MHC-fed rat hippocampus appeared as increased TUNEL staining and higher caspase-3 activity. Similar observations are common in recent literature whereby neuroinflammation and microglial activation [78–80], together with hippocampal apoptosis [81,82], occur in association with high fat diet-induced cognitive decline. The previous studies provided observational evidence for the aforementioned association. However, in the context of the current study, it is possible that the impeded autophagic flux in MHC-fed rat hippocampus was the trigger for activation of apoptosis and inflammation as previously observed in neuronal and non-neuronal tissues [83–85].

From a different perspective, our previous work showed that the amelioration of adipose inflammation in this rat model of early metabolic challenge was associated with reversal of the vascular dysfunction *in vitro* and *in vivo* [31,32]. In the present study, the same non-hypoglycemic doses of metformin and pioglitazone used to ameliorate adipose inflammation in the previous work led to improved

cerebrovascular function. This was also associated with an improved performance in MWM and Y-maze tests. The only metabolic impact was observed in the pioglitazone-treated group as a reduction of serum insulin level, consistent with its insulin-sensitizing effect. Nevertheless, a large body of literature support a direct ameliorative impact of metformin and pioglitazone on vascular endothelial dysfunction in patients with metabolic syndrome, prediabetes, and diabetes [86–88]. Despite the lack of a detectable change in HIF-1 α expression levels, improvement of cerebrovascular function in the treated groups was associated with favorable changes in the mitochondrial markers, DRP1 phosphorylation and Sirt3 expression, as well as with reduced oxidative stress. While presumed to be related to brain perfusion, an absence of a detectable decrease in HIF-1 α expression level is not unexpected given that prior studies on diabetic rat models showed that significant changes were only observed after at least one month of intervention [89]. Nevertheless, treatment by metformin and pioglitazone reversed the molecular changes in the pathways leading to suppression of autophagy. While a reduction in Akt phosphorylation, and the subsequent mTORC activation, are consistent with reduced serum insulin levels in the pioglitazone-treated MHC-fed rat group, prior evidence reported a direct inhibitory effect for metformin on Akt, as well as mTORC, phosphorylation and activation [90]. This was associated with a reversal of the changes seen in the autophagy markers p62 and LC3. Along the same lines, the CA1 area of the hippocampus in metformin- and pioglitazone-treated MHC rats showed reduced markers of microglial activation and apoptosis.

While our results argue for metabolic impairment as the underlying cause of the present observations, some studies report a direct inhibitory effect of free fatty acids on vascular endothelial reactivity [91]. Indeed, serum free fatty acids increase in high-fat fed rodents [92]. As such, while unlikely, changes in dietary composition cannot be completely ruled out as a cause of the present observations, at least in the context of triggering endothelial dysfunction and increased cerebrovascular reactivity.

In conclusion, the results of the present study offer a plausible framework for a continuum of events linking peripheral inflammatory changes in early metabolic dysfunction to cognitive decline (summarized in Fig. 7). Cerebrovascular changes, occurring in the context of

wider vascular dysfunction secondary to metabolic alteration, lead to hippocampal hypoxia with possible mitochondrial dysfunction and increased oxidative stress. In parallel, the altered metabolic profile potentially contributes to a reduced autophagic flux precluding the neuronal rescue mechanism, and thus leads to the activation of apoptosis and neuroinflammation observed alongside cognitive impairment in this model. Amelioration of the peripheral inflammatory process improves vascular, molecular, and behavioral alterations highlighting both the feasibility and importance of intervention to reverse the cognitive impact of this early stage of metabolic dysfunction.

CRedit authorship contribution statement

Walaah Fakh: Investigation, Writing - original draft. **Ali Mroueh:** Investigation. **Houssein Salah:** Investigation. **Ali H. Eid:** Resources, Writing - review & editing. **Makram Obeid:** Methodology, Resources, Writing - review & editing. **Firas Kobeissy:** Funding acquisition, Resources, Writing - review & editing. **Hala Darwish:** Methodology, Formal analysis, Funding acquisition, Writing - review & editing. **Ahmed F. El-Yazbi:** Conceptualization, Methodology, Formal analysis, Resources, Writing - original draft, Writing - review & editing, Visualization, Supervision, Project administration, Funding acquisition.

Declaration of Competing Interest

The authors declare that they have no known competing financial interests or personal relationships that could have appeared to influence the work reported in this paper.

Acknowledgements

This study was supported by a grant (number 010817) jointly funded by the National Council for Scientific Research in Lebanon (CNRS-L) and the American University of Beirut (AUB) granted to AFE. The funding bodies had no role in the design of the study or collection, analysis, and interpretation of data or in writing the manuscript.

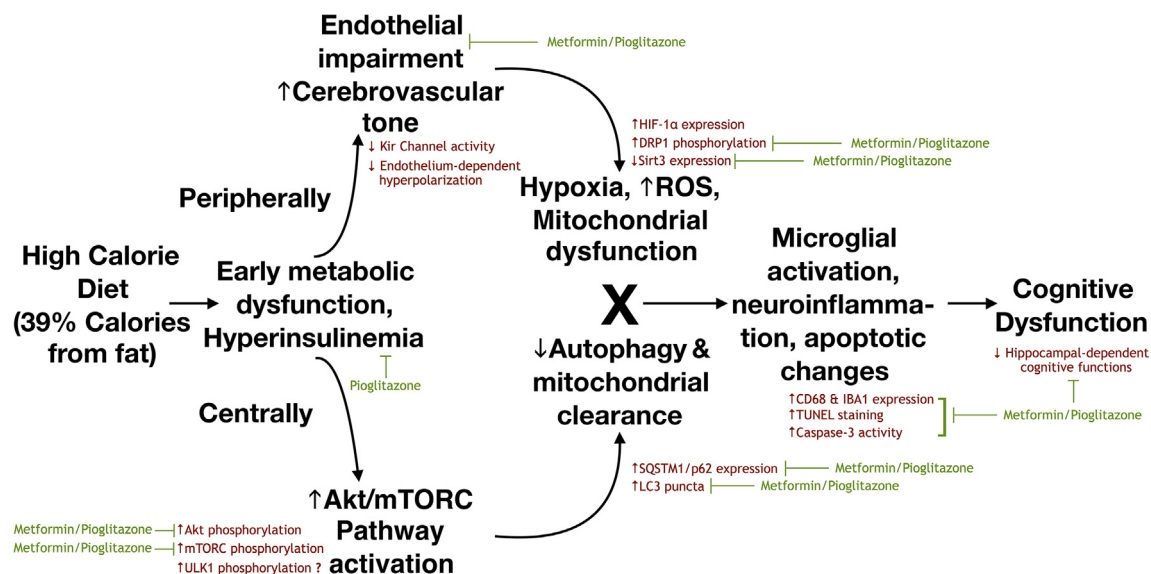


Fig. 7. The hypothesized mechanistic scheme linking early prediabetes to cognitive dysfunction. Early metabolic impairment is associated with endothelial dysfunction and increased cerebrovascular tone. This leads to a chronic state of mild hypoxia leading to mitochondrial stress and increased reactive oxygen species production. On the other hand, hyperinsulinemia developing at this early stage suppresses the autophagic flux through the Akt/mTOR pathway precluding possible neuronal rescue. Both factors could possibly converge into neuronal inflammation and neuronal cell death, which might underlie the observed cognitive decline in this rat model. Metformin and pioglitazone alleviate the metabolic dysfunction improving vascular reactivity and also improve hyperinsulinemia (pioglitazone) or interfere with insulin signaling (metformin) ameliorating both pathways leading to neuronal damage and cognitive impairment.

References

- [1] International Diabetes Federation, IDF Diabetes Atlas, ninth ed., International Diabetes Federation, Brussels, Belgium, 2019.
- [2] H.V. Kuhnlein, O. Receveur, Dietary change and traditional food systems of indigenous peoples, *Annu. Rev. Nutr.* 16 (1996) 417–442.
- [3] A. Misra, N. Singhal, L. Khurana, Obesity, the metabolic syndrome, and type 2 diabetes in developing countries: role of dietary fats and oils, *J. Am. Coll. Nutr.* 29 (3 Suppl) (2010) 289S–301S.
- [4] B.M. Leon, T.M. Maddox, Diabetes and cardiovascular disease: epidemiology, biological mechanisms, treatment recommendations and future research, *World J. Diabetes* 6 (13) (2015) 1246–1258.
- [5] A. Marseglia, L. Fratiglioni, G. Kalpouzos, R. Wang, L. Backman, W. Xu, Prediabetes and diabetes accelerate cognitive decline and predict microvascular lesions: a population-based cohort study, *Alzheimer's Dementia* 15 (1) (2019) 25–33.
- [6] T.M. Hughes, S. Craft, The role of insulin in the vascular contributions to age-related dementia, *Biochim. Biophys. Acta (BBA) – Mol. Basis Dis.* 1862 (5) (2016) 983–991.
- [7] A.G. Tabak, C. Herder, W. Rathmann, E.J. Brunner, M. Kivimaki, Prediabetes: a high-risk state for diabetes development, *Lancet (London, England)* 379 (9833) (2012) 2279–2290.
- [8] G. Cheng, C. Huang, H. Deng, H. Wang, Diabetes as a risk factor for dementia and mild cognitive impairment: a meta-analysis of longitudinal studies, *Int. Med. J.* 42 (5) (2012) 484–491.
- [9] M. Buysschaert, J.L. Medina, M. Bergman, A. Shah, J. Lonier, Prediabetes and associated disorders, *Endocrine* 48 (2) (2015) 371–393.
- [10] R.H. Tuligenga, A. Dugravot, A.G. Tabák, A. Elbaz, E.J. Brunner, M. Kivimäki, A. Singh-Manoux, Midlife type 2 diabetes and poor glycaemic control as risk factors for cognitive decline in early old age: a post-hoc analysis of the Whitehall II cohort study, *Lancet Diabetes Endocrinol.* 2 (3) (2014) 228–235.
- [11] E. Dybjer, P.M. Nilsson, G. Engström, C. Helmer, K. Nägga, Pre-diabetes and diabetes are independently associated with adverse cognitive test results: a cross-sectional, population-based study, *BMC Endocr. Disord.* 18 (1) (2018) 91.
- [12] M. Lutski, G. Weinstein, U. Goldbourt, D. Tanne, Insulin resistance and future cognitive performance and cognitive decline in elderly patients with cardiovascular disease, *J. Alzheimer's Dis.* 57 (2) (2017) 633–643.
- [13] C.T. Kodl, E.R. Seaquist, Cognitive dysfunction and diabetes mellitus, *Endocr. Rev.* 29 (4) (2008) 494–511.
- [14] P. Van Dyken, B. Lacoste, Impact of metabolic syndrome on neuroinflammation and the blood-brain barrier, *Front. Neurosci.* 12 (2018) 930–930.
- [15] G.J. Biessels, A.C. Kappelle, B. Bravenboer, D.W. Erkelens, W.H. Gispen, Cerebral function in diabetes mellitus, *Diabetologia* 37 (7) (1994) 643–650.
- [16] A. Ergul, A. Kelly-Cobbs, M. Abdalla, S.C. Fagan, Cerebrovascular complications of diabetes: focus on stroke, *Endocr. Metab. Immune Disord. Drug Targets* 12 (2) (2012) 148–158.
- [17] H. Rusinek, J. Ha, P.L. Yau, P. Storey, A. Tirsi, W.H. Tsui, O. Frosch, S. Azova, A. Convit, Cerebral perfusion in insulin resistance and type 2 Diabetes, *J. Cereb. Blood Flow Metab.* 35 (1) (2015) 95–102.
- [18] K.S. Abd-Elrahman, O. Colinas, E.J. Walsh, H.L. Zhu, C.M. Campbell, M.P. Walsh, W.C. Cole, Abnormal myosin phosphatase targeting subunit 1 phosphorylation and actin polymerization contribute to impaired myogenic regulation of cerebral arterial diameter in the type 2 diabetic Goto-Kakizaki rat, *J. Cerebral Blood Flow Metab.* 37 (1) (2017) 227–240.
- [19] J.T. Butcher, A.G. Goodwill, S.C. Stanley, J.C. Frisbee, Differential impact of dilator stimuli on increased myogenic activation of cerebral and skeletal muscle resistance arterioles in obese Zucker rats, *Microcirculation (New York, N.Y.: 1994)* 20 (7) (2013) 579–589.
- [20] M. Glatigny, S. Moriceau, M. Rivagorda, M. Ramos-Brossier, A.C. Nascimbeni, F. Lante, M.R. Shanley, N. Boudarene, A. Rousseaud, A.K. Friedman, C. Settembre, N. Kuperwasser, G. Friedlander, A. Buisson, E. Morel, P. Codogno, F. Oury, Autophagy is required for memory formation and reverses age-related memory decline, *Curr. Biol.* 29 (3) (2019) 435–448.e8.
- [21] J.H. Son, J.H. Shim, K.-H. Kim, J.-Y. Ha, J.Y. Han, Neuronal autophagy and neurodegenerative diseases, *Exp. Mol. Med.* 44 (2012) 89.
- [22] A. Tramutola, J.C. Triplett, F. Di Domenico, D.M. Niedowicz, M.P. Murphy, R. Coccia, M. Perluigi, D.A. Butterfield, Alteration of mTOR signaling occurs early in the progression of Alzheimer disease (AD): analysis of brain from subjects with pre-clinical AD, amnesic mild cognitive impairment and late-stage AD, *J. Neurochem.* 133 (5) (2015) 739–749.
- [23] Y.D. Kim, E.I. Jeong, J. Nah, S.-M. Yoo, W.J. Lee, Y. Kim, S. Moon, S.-H. Hong, Y.-K. Jung, Pimozide reduces toxic forms of tau in TauC3 mice via 5' adenosine monophosphate-activated protein kinase-mediated autophagy, *J. Neurochem.* 142 (5) (2017) 734–746.
- [24] K.S. Abd-Elrahman, A. Hamilton, S.R. Hutchinson, F. Liu, R.C. Russell, S.S.G. Ferguson, mGluR5 antagonism increases autophagy and prevents disease progression in the zQ175 mouse model of Huntington's disease, *Sci. Signal.* 10 (510) (2017).
- [25] T. Hara, K. Nakamura, M. Matsui, A. Yamamoto, Y. Nakahara, R. Suzuki-Migishima, M. Yokoyama, K. Mishima, I. Saito, H. Okano, N. Mizushima, Suppression of basal autophagy in neural cells causes neurodegenerative disease in mice, *Nature* 441 (7095) (2006) 885–889.
- [26] H.Y. Liu, J. Han, S.Y. Cao, T. Hong, D. Zhuo, J. Shi, Z. Liu, W. Cao, Hepatic autophagy is suppressed in the presence of insulin resistance and hyperinsulinemia: inhibition of FoxO1-dependent expression of key autophagy genes by insulin, *J. Biol. Chem.* 284 (45) (2009) 31484–31492.
- [27] C. He, M.C. Bassik, V. Moresi, K. Sun, Y. Wei, Z. Zou, Z. An, J. Loh, J. Fisher, Q. Sun, S. Korsmeyer, M. Packer, H.I. May, J.A. Hill, H.W. Virgin, C. Gilpin, G. Xiao, R. Bassel-Duby, P.E. Scherer, B. Levine, Exercise-induced BCL2-regulated autophagy is required for muscle glucose homeostasis, *Nature* 481 (7382) (2012) 511–515.
- [28] M. Vandal, P.J. White, C. Tremblay, I. St-Amour, G. Chevrier, V. Emond, D. Lefrançois, J. Virgili, E. Planel, Y. Giguere, A. Marette, F. Calon, Insulin reverses the high-fat diet-induced increase in brain Abeta and improves memory in an animal model of Alzheimer disease, *Diabetes* 63 (12) (2014) 4291–4301.
- [29] O. Busquets, M. Etcheto, M. Pallas, C. Beas-Zarate, E. Verdaguier, C. Auladell, J. Folch, A. Camins, Long-term exposition to a high fat diet favors the appearance of beta-amyloid depositions in the brain of C57BL/6J mice. A potential model of sporadic Alzheimer's disease, *Mech. Ageing Dev.* 162 (2017) 38–45.
- [30] M. Takalo, A. Haapasalo, H. Martiskainen, K.M. Kurkinen, H. Koivisto, P. Miettinen, V.K. Khandelwal, S. Kemppainen, D. Kaminska, P. Makinen, V. Leinonen, J. Pihlajamaki, H. Soininen, M. Laakso, H. Tanila, M. Hiltunen, High-fat diet increases tau expression in the brain of T2DM and AD mice independently of peripheral metabolic status, *J. Nutr. Biochem.* 25 (6) (2014) 634–641.
- [31] O. Al-Assi, R. Ghali, A. Mroueh, A. Kaplan, N. Mougharbil, A.H. Eid, F.A. Zouein, A. El-Yazbi, Cardiac autonomic neuropathy as a result of mild hypercaloric challenge in absence of signs of diabetes: modulation by antidiabetic drugs, *Oxid. Med. Cell Longev.* 2018 (2018) 9389784.
- [32] M.A.W. Elkhatib, A. Mroueh, R.W. Rafef, F. Sleiman, H. Fouad, E.I. Saad, M.A. Fouda, O. Elgaddar, K. Issa, A.H. Eid, A.A. Eid, K.S. Abd-Elrahman, A.F. El-Yazbi, Amelioration of perivascular adipose inflammation reverses vascular dysfunction in a model of nonobese prediabetic metabolic challenge: potential role of antidiabetic drugs, *Transl. Res.* (2019).
- [33] R. Alaaeddine, M. El-Khatib, A. Mroueh, H. Fouad, E. Saad, M. El-Sabban, F. Plane, A. El-Yazbi, Impaired endothelium-dependent hyperpolarization underlies endothelial dysfunction during early metabolic challenge: Increased ROS generation and possible interference with NO function, *J. Pharmacol. Exp. Ther.* (2019) jpet.119.262048.
- [34] C. National Research Council Committee for the Update of the Guide for the, A. Use of Laboratory, The National Academies Collection: Reports funded by National Institutes of Health, in: th (Ed.), *Guide for the Care and Use of Laboratory Animals*, National Academies Press (US), National Academy of Sciences, Washington (DC), 2011.
- [35] P.G. Reeves, F.H. Nielsen, G.C. Fahey Jr., AIN-93 purified diets for laboratory rodents: final report of the American Institute of Nutrition ad hoc writing committee on the reformulation of the AIN-76A rodent diet, *J. Nutr.* 123 (11) (1993) 1939–1951.
- [36] T.L. Davidson, A. Monnot, A.U. Neal, A.A. Martin, J.J. Horton, W. Zheng, The effects of a high-energy diet on hippocampal-dependent discrimination performance and blood-brain barrier integrity differ for diet-induced obese and diet-resistant rats, *Physiol. Behav.* 107 (1) (2012) 26–33.
- [37] T.L. Davidson, S.L. Hargrave, S.E. Swithers, C.H. Sample, X. Fu, K.P. Kinzig, W. Zheng, Inter-relationships among diet, obesity and hippocampal-dependent cognitive function, *Neuroscience* 253 (2013) 110–122.
- [38] C.J. Miedel, J.M. Patton, A.N. Miedel, E.S. Miedel, J.M. Levenson, Assessment of spontaneous alternation, novel object exploration and limb clasping in transgenic mouse models of amyloid-beta and tau neuropathology, *J. Visualized Experiments: JoVE* (123) (2017).
- [39] T.L. Briones, H. Darwish, Vitamin D mitigates age-related cognitive decline through the modulation of pro-inflammatory state and decrease in amyloid burden, *J. Neuroinflamm.* 9 (2012) 244.
- [40] Y. Medlej, H. Salah, L. Wadi, S. Saad, B. Bashir, J. Allam, Z. Atoui, N. Darwish, N. Karnib, H. Darwish, F. Kobeissy, K.K.W. Wang, E. Hamade, M. Obeid, Lestaurinib (CEP-701) modulates the effects of early life hypoxic seizures on cognitive and emotional behaviors in immature rats, *Epilepsy Behav.* 92 (2019) 332–340.
- [41] A. Manaenko, H. Chen, J. Kammer, J.H. Zhang, J. Tang, Comparison Evans Blue injection routes: intravenous versus intraperitoneal, for measurement of blood-brain barrier in a mice hemorrhage model, *J. Neurosci. Methods* 195 (2) (2011) 206–210.
- [42] A.L. Salgado, L. Carvalho, A.C. Oliveira, V.N. Santos, J.G. Vieira, E.R. Parise, Insulin resistance index (HOMA-IR) in the differentiation of patients with non-alcoholic fatty liver disease and healthy individuals, *Arq. Gastroenterol.* 47 (2) (2010) 165–169.
- [43] A.C. Ocampo, L.R. Squire, R.E. Clark, Hippocampal area CA1 and remote memory in rats, *Learn. Memory (Cold Spring Harbor, N.Y.)* 24 (11) (2017) 563–568.
- [44] M.C. Larkin, C. Lykken, L.D. Tye, J.G. Wickelgren, L.M. Frank, Hippocampal output area CA1 broadcasts a generalized novelty signal during an object-place recognition task, *Hippocampus* 24 (7) (2014) 773–783.
- [45] A.F. El-Yazbi, W.J. Cho, R. Schulz, E.E. Daniel, Caveolin-1 knockout alters beta-adrenoceptors function in mouse small intestine, *Am. J. Physiol. Gastrointest. Liver Physiol.* 291 (6) (2006) G1020–G1030.
- [46] A.F. El-Yazbi, K.S. Ibrahim, H.M. El-Gowell, N.M. El-Deeb, M.M. El-Mas, Modulation by NADPH oxidase of the chronic cardiovascular and autonomic interaction between cyclosporine and NSAIDs in female rats, *Eur. J. Pharmacol.* 806 (2017) 96–104.
- [47] R.M. Memmott, P.A. Dennis, Akt-dependent and-independent mechanisms of mTOR regulation in cancer, *Cell. Signal.* 21 (5) (2009) 656–664.
- [48] U. Hostalek, Global epidemiology of prediabetes – present and future perspectives, *Clin. Diab. Endocrinol.* 5 (2019) 5.
- [49] A.B. Evert, J.L. Boucher, M. Cypress, S.A. Dunbar, M.J. Franz, E.J. Mayer-Davis, J.J. Neumiller, R. Nwankwo, C.L. Verdi, P. Urbanski, W.S. Yancy Jr., Nutrition

- therapy recommendations for the management of adults with diabetes, *Diabetes Care* 37 (Suppl 1) (2014) S120–S143.
- [50] P. Valensi, Hypertension, single sugars and fatty acids, *J. Hum. Hypertens.* 19 (Suppl 3) (2005) S5–S9.
- [51] G.C. Weir, S. Bonner-Weir, Five stages of evolving beta-cell dysfunction during progression to diabetes, *Diabetes* 53 (suppl 3) (2004) S16–S21.
- [52] L. Forny-Germano, F.G. De Felice, M. Vieira, The role of leptin and adiponectin in obesity-associated cognitive decline and Alzheimer's disease, *Front. Neurosci.* 12 (2018) 1027.
- [53] A.F. El-Yazbi, K.S. Abd-Elrahman, ROK and arteriolar myogenic tone generation: molecular evidence in health and disease, *Front. Pharmacol.* 8 (2017) 87.
- [54] D.D. Heistad, What's new in the cerebral microcirculation? Landis award lecture, *Microcirculation* (New York, N.Y.: 1994) 8 (6) (2001) 365–375.
- [55] A. Arias-Cavieres, M.A. Khuu, C.U. Nwakudu, J.E. Barnard, G. Dalgin, A.J. Garcia, A role for hypoxia inducible factor 1a (HIF1a) in intermittent hypoxia-dependent changes to spatial memory and synaptic plasticity, *bioRxiv* (2019) 595975.
- [56] R. Chen, U.H. Lai, L. Zhu, A. Singh, M. Ahmed, N.R. Forsyth, Reactive oxygen species formation in the brain at different oxygen levels: the role of hypoxia inducible factors, *Front. Cell Dev. Biol.* 6 (2018) 132.
- [57] X.Y. Zhao, M.H. Lu, D.J. Yuan, D.E. Xu, P.P. Yao, W.L. Ji, H. Chen, W.L. Liu, C.X. Yan, Y.Y. Xia, S. Li, J. Tao, Q.H. Ma, Mitochondrial dysfunction in neural injury, *Front. Neurosci.* 13 (2019) 30.
- [58] C.R. Chang, C. Blackstone, Dynamic regulation of mitochondrial fission through modification of the dynamin-related protein Drp1, *Ann. NY. Acad. Sci.* 1201 (2010) 34–39.
- [59] E. Sidorova-Darmos, R. Sommer, J.H. Eubanks, The role of SIRT3 in the brain under physiological and pathological conditions, *Front. Cell. Neurosci.* 12 (196) (2018).
- [60] J. Ježek, K.F. Cooper, R. Strich, Reactive oxygen species and mitochondrial dynamics: the yin and yang of mitochondrial dysfunction and cancer progression, *Antioxidants* (Basel, Switzerland) 7 (1) (2018) 13.
- [61] L.W. Thomas, M. Ashcroft, Exploring the molecular interface between hypoxia-inducible factor signalling and mitochondria, *Cell. Mol. Life Sci.* 76 (9) (2019) 1759–1777.
- [62] D. Zhang, Y. Liu, Y. Tang, X. Wang, Z. Li, R. Li, Z. Ti, W. Gao, J. Bai, Y. Lv, Increased mitochondrial fission is critical for hypoxia-induced pancreatic beta cell death, *PLoS One* 13 (5) (2018) e0197266.
- [63] C.W. Kuo, M.H. Tsai, T.K. Lin, M.M. Tiao, P.W. Wang, J.H. Chuang, S.D. Chen, C.W. Liou, mtDNA as a mediator for expression of hypoxia-inducible factor 1alpha and ROS in hypoxic neuroblastoma cells, *Int. J. Mol. Sci.* 18 (6) (2017).
- [64] D.Y. Kim, S.Y. Jung, Y.J. Kim, S. Kang, J.H. Park, S.T. Ji, W.B. Jang, S. Lamichane, B.D. Lamichane, Y.C. Chae, D. Lee, J.S. Chung, S.-M. Kwon, Hypoxia-dependent mitochondrial fission regulates endothelial progenitor cell migration, invasion, and tube formation, *Korean J. Physiol. Pharmacol.* 22 (2) (2018) 203–213.
- [65] Z. Shi, C. Li, Y. Yin, Z. Yang, H. Xue, N. Mu, Y. Wang, M. Liu, H. Ma, Aerobic interval training regulated SIRT3 attenuates high-fat-diet-associated cognitive dysfunction, *Biomed Res. Int.* 2018 (2018) 2708491–2708491.
- [66] J. Balog, S.L. Mehta, R. Vemuganti, Mitochondrial fission and fusion in secondary brain damage after CNS insults, *J. Cereb. Blood Flow Metab.* 36 (12) (2016) 2022–2033.
- [67] G. Twig, A. Elorza, A.J. Molina, H. Mohamed, J.D. Wikstrom, G. Walzer, L. Stiles, S.E. Haigh, S. Katz, G. Las, J. Alroy, M. Wu, B.F. Py, J. Yuan, J.T. Deeney, B.E. Corkey, O.S. Shirihai, Fission and selective fusion govern mitochondrial segregation and elimination by autophagy, *EMBO J.* 27 (2) (2008) 433–446.
- [68] H. Chen, D.C. Chan, Mitochondrial dynamics—fusion, fission, movement, and mitophagy—in neurodegenerative diseases, *Hum. Mol. Genet.* 18 (R2) (2009) R169–R176.
- [69] J. Puyal, V. Ginet, Y. Grishchuk, A.C. Truttmann, P.G.H. Clarke, Neuronal autophagy as a mediator of life and death: contrasting roles in chronic neurodegenerative and acute neural disorders, *Neuroscientist* 18 (3) (2012) 224–236.
- [70] Z.Y. Shi, J.X. Deng, S. Fu, L. Wang, Q. Wang, B. Liu, Y.Q. Li, J.B. Deng, Protective effect of autophagy in neural ischemia and hypoxia: Negative regulation of the Wnt/beta-catenin pathway, *Int. J. Mol. Med.* 40 (6) (2017) 1699–1708.
- [71] W. Balduini, S. Carloni, G. Buonocore, Autophagy in hypoxia-ischemia induced brain injury, *J. Maternal-Fetal Neonatal Med.* 25 (supl) (2012) 30–34.
- [72] N.P. de Mello, A.M. Orellana, C.H. Mazucanti, G. de Moraes Lima, C. Scavone, E.M. Kawamoto, Insulin and autophagy in neurodegeneration, *Front. Neurosci.* 13 (491) (2019).
- [73] S.E. Ehrlicher, H.D. Stierwalt, S.A. Newsom, M.M. Robinson, Skeletal muscle autophagy remains responsive to hyperinsulinemia and hyperglycemia at higher plasma insulin concentrations in insulin-resistant mice, *Physiol. Rep.* 6 (14) (2018) e13810.
- [74] M. Paquette, L. El-Houjeiri, A. Pause, mTOR pathways in cancer and autophagy, *Cancers* 10 (1) (2018).
- [75] C. Wang, H. Wang, D. Zhang, W. Luo, R. Liu, D. Xu, L. Diao, L. Liao, Z. Liu, Phosphorylation of ULK1 affects autophagosome fusion and links chaperone-mediated autophagy to macroautophagy, *Nat. Commun.* 9 (1) (2018) 3492.
- [76] M. Bordi, M.J. Berg, P.S. Mohan, C.M. Peterhoff, M.J. Alldred, S. Che, S.D. Ginsberg, R.A. Nixon, Autophagy flux in CA1 neurons of Alzheimer hippocampus: increased induction overburdens failing lysosomes to propel neuritic dystrophy, *Autophagy* 12 (12) (2016) 2467–2483.
- [77] D.A.E. Hendrickx, C.G. van Eden, K.G. Schuurman, J. Hamann, I. Huitinga, Staining of HLA-DR, Iba1 and CD68 in human microglia reveals partially overlapping expression depending on cellular morphology and pathology, *J. Neuroimmunol.* 309 (2017) 12–22.
- [78] C.M. Duffy, J.J. Hofmeister, J.P. Nixon, T.A. Butterick, High fat diet increases cognitive decline and neuroinflammation in a model of orexin loss, *Neurobiol. Learn. Mem.* 157 (2019) 41–47.
- [79] S.J. Spencer, H. D'Angelo, A. Soch, L.R. Watkins, S.F. Maier, R.M. Barrientos, High-fat diet and aging interact to produce neuroinflammation and impair hippocampal- and amygdala-dependent memory, *Neurobiol. Aging* 58 (2017) 88–101.
- [80] Y. Duan, L. Zeng, C. Zheng, B. Song, F. Li, X. Kong, K. Xu, Inflammatory links between high fat diets and diseases, *Front. Immunol.* 9 (2649) (2018).
- [81] S. Nakandakari, V.R. Munoz, G.K. Kuga, R.C. Gaspar, M.R. Sant'Ana, I.C.B. Pavan, L.G.S. da Silva, A.P. Morelli, F.M. Simabuco, A.S.R. da Silva, L.P. de Moura, E.R. Ropelle, D.E. Cintra, J.R. Pauli, Short-term high-fat diet modulates several inflammatory, ER stress, and apoptosis markers in the hippocampus of young mice, *Brain Behav. Immun.* 79 (2019) 284–293.
- [82] S. Qin, D. Sun, C. Zhang, Y. Tang, F. Zhou, K. Zheng, R. Tang, Y. Zheng, Downregulation of sonic hedgehog signaling in the hippocampus leads to neuronal apoptosis in high-fat diet-fed mice, *Behav. Brain Res.* 367 (2019) 91–100.
- [83] G. Mariño, M. Niso-Santano, E.H. Baehrecke, G. Kroemer, Self-consumption: the interplay of autophagy and apoptosis, *Nat. Rev. Mol. Cell Biol.* 15 (2) (2014) 81–94.
- [84] H. Wei, M. Yin, Y. Lu, Y. Yang, B. Li, X.-X. Liao, G. Dai, X. Jing, Y. Xiong, C. Hu, Mild hypothermia improves neurological outcome in mice after cardiopulmonary resuscitation through silent information regulator 1-activated autophagy, *Cell Death Discov.* 5 (2019) 129–129.
- [85] J. Chen, L. Wang, C. Wu, Q. Hu, C. Gu, F. Yan, J. Li, W. Yan, G. Chen, Melatonin-enhanced autophagy protects against neural apoptosis via a mitochondrial pathway in early brain injury following a subarachnoid hemorrhage, *J. Pineal Res.* 56 (1) (2014) 12–19.
- [86] J. Xu, M.H. Zou, Molecular insights and therapeutic targets for diabetic endothelial dysfunction, *Circulation* 120 (13) (2009) 1266–1286.
- [87] S. Rizza, M. Cardellini, O. Porzio, C. Pecchioli, A. Savo, I. Cardolini, N. Senese, D. Lauro, P. Sbraccia, R. Lauro, M. Federici, Pioglitazone improves endothelial and adipose tissue dysfunction in pre-diabetic CAD subjects, *Atherosclerosis* 215 (1) (2011) 180–183.
- [88] C.R. Triggle, H. Ding, Metformin is not just an antihyperglycaemic drug but also has protective effects on the vascular endothelium, *Acta Physiol.* 219 (1) (2017) 138–151.
- [89] L. Gu, H. Xu, C. Zhang, Q. Yang, L. Zhang, J. Zhang, Time-dependent changes in hypoxia- and gliosis-related factors in experimental diabetic retinopathy, *Eye* (London) 33 (4) (2019) 600–609.
- [90] R. Würth, A. Pattarozzi, M. Gatti, A. Bajetto, A. Corsaro, A. Parodi, R. Sirtito, M. Massollo, C. Marini, G. Zona, D. Fenoglio, G. Sambucetti, G. Filaci, A. Daga, F. Barbieri, T. Florio, Metformin selectively affects human glioblastoma tumor-initiating cell viability, *Cell Cycle* 12 (1) (2013) 145–156.
- [91] I. Edirisinghe, K. McCormick Hallam, C.T. Kappagoda, Effect of fatty acids on endothelium-dependent relaxation in the rabbit aorta, *Clin. Sci.* 111 (2) (2006) 145–151.
- [92] M. Yamato, T. Shiba, M. Yoshida, T. Ide, N. Seri, W. Kudou, S. Kinugawa, H. Tsutsui, Fatty acids increase the circulating levels of oxidative stress factors in mice with diet-induced obesity via redox changes of albumin, *FEBS J.* 274 (15) (2007) 3855–3863.